LETTERS

# Seasonal dynamics of recurrent epidemics

Lewi Stone[1,2]*, Ronen Olinky[1]* & Amit Huppert[1,2]*

**Seasonality is a driving force that has a major effect on the spatio-temporal dynamics of natural systems and their populations[1–5]. This is especially true for the transmission of common infectious diseases (such as influenza, measles, chickenpox and pertussis), and is of great relevance for host–parasite relationships in general[1–23]. Here we gain further insights into the nonlinear dynamics of recurrent diseases through the analysis of the classical seasonally forced SIR (susceptible, infectious or recovered) epidemic model[6,7]. Our analysis differs from other modelling studies in that the focus is more on post-epidemic dynamics than the outbreak itself. Despite the mathematical intractability of the forced SIR model, we identify a new threshold effect and give clear analytical conditions for predicting the occurrence of either a future epidemic outbreak, or a 'skip'—a year in which an epidemic fails to initiate. The threshold is determined by the population's susceptibility measured after the last outbreak and the rate at which new susceptible individuals are recruited into the population. Moreover, the time of occurrence (that is, the phase) of an outbreak proves to be a useful parameter that carries important epidemiological information. In forced systems, seasonal changes can prevent late-peaking diseases (that is, those having high phase) from spreading widely, thereby increasing population susceptibility, and controlling the triggering and intensity of future epidemics. These principles yield forecasting tools that should have relevance for the study of newly emerging and re-emerging diseases controlled by seasonal vectors.**

The strong effect of seasonality on population dynamics is no better seen than in the historical long-term data sets of seasonally recurring childhood infectious diseases, such as measles, mumps and chickenpox. These diseases are driven by the seasonally changing contact rate between children which increases sharply at the beginning of each school year, and strongly controls the ensuing disease transmission. Figure 1a, c displays two time series of reported cases of measles in New York (1928–64) and London (1948–68) in the pre-vaccination era[4–6]. Major epidemics peak close to Spring each year, and on many occasions every second year if the dynamics are biennial and the outbreak 'skips' a year. Note there is also a strong erratic and possibly chaotic component, as seen in the variability of peak heights of the epidemics, as well as the intermittent jumps between periods of annual and biennial dynamics[4–12]. Theoretical studies have shown that seasonal forcing can be responsible for inducing similar complex population dynamics such as higher-order cycles, resonances and deterministic chaos[6,7,10–26]. These complex responses can easily mask any simple underlying mechanistic processes that might otherwise help in forecasting future epidemics (Fig. 1 legend). The modelling framework used here helps uncover, and gives new insights into, these processes.

The driving force maintaining recurrent epidemic dynamics has long been recognized to be the continuous birth and recruitment of new susceptible individuals into the population[1,5,6,25]. As an outbreak progresses, susceptibles ($S$) become infected, drop to a minimum level ($S_0$) in the wake of the epidemic, and then grow in number as the birth process begins to dominate once again. The pattern of epidemics from year to year is controlled by the population's periodically changing annual contact rate. Our mathematical analysis has shown it useful to focus on $S_0$, defined as the local minimum number of susceptibles left in the wake of an epidemic. $S_0$ controls whether there will be an outbreak in the year ahead or the number of ensuing skips that follow. To a good approximation, we have shown that to generate $k$ or more consecutive skips in successive years requires that $S_0$ fall below:

$$S_c(k) = \frac{\gamma+\mu}{\beta_0} - \frac{(k+1)\mu\chi}{2} \quad (1)$$

The critical threshold is defined in terms of classical epidemiological parameters: $\gamma$ represents the rate at which infected individuals recover;

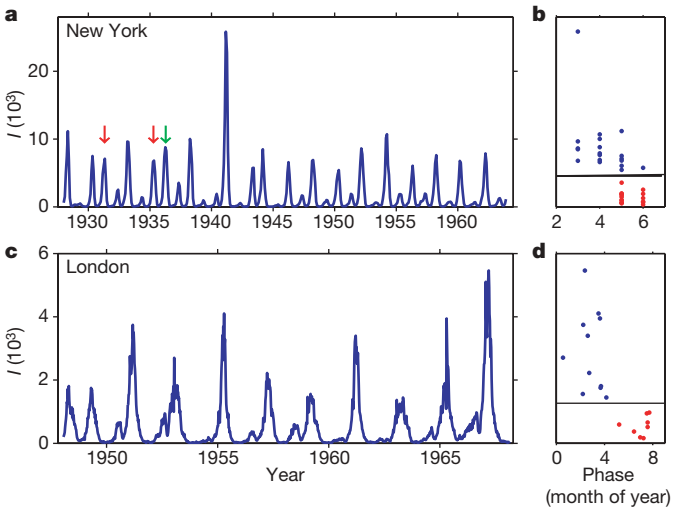


**Figure 1 | Epidemic time series together with their associated phase relationship and synchronization effects.** **a**, **c**, Time series of reported measles infective cases ($I$, in thousands) from the largest city in the US (New York, monthly sampling) and in the UK (London, weekly sampling) in the pre-vaccination era (see Methods). **b**, **d**, The maximum number of infectives of each epidemic is plotted as a function of the time of year (phase in months) at which this maximum occurred. Minor epidemic peaks (skips) have been plotted in red to emphasize that all skips occur at the end of the 'high' season, and are thus synchronized (see text). The probability of finding all red points only in the late phase regime is $P < 0.001$, making the synchronization significant. Limitations of conventional prediction schemes are as follows. Consider the New York time-series (**a**) where two similar sized 'intermediate' outbreaks occurred in 1931 and 1935 (red arrows). The former was followed by a skip, whereas the latter was followed by another intermediate outbreak in 1936 (green arrow). Given the very different outcomes, peak-to-peak predictions become untenable. The problem intensifies when trying to predict outbreaks that occur after skips. The latter skips can be followed by a variety of different sized peaks, ranging from a successive skip (for example, New York in 1940) to extremely large epidemics (for example, New York in 1941).

[1]Biomathematics Unit, Department of Zoology, Faculty of Life Science, [2]The Porter School of Environmental Studies, Tel Aviv University, Ramat Aviv 69978, Israel.
*These authors contributed equally to this work.

$\mu$ is the per capita rate at which members of the population reproduce and die; and $\beta_0$ is the rate of effective contacts between infected and susceptible individuals averaged over the year. The seasonal forcing modulates the contact rate and is taken to be annual with period $\chi = 1$ ($\chi$ having time units of years). For example, the commonly used sinusoidally forced contact rate changes annually in time ($t$) according to the relation $\beta(t) = \beta_0[1 + \delta\sin(2\pi t)]$, with $\delta$ setting the strength of the forcing. The mathematical derivation of the threshold is given in Supplementary Information B and C, and is based on an analysis of the model's post-epidemic dynamics in the phase plane (Fig. 2a and Methods). More specifically, for $k = 0$, one obtains:

$$S_0 > S_c = \frac{\gamma+\mu}{\beta_0} - \frac{\mu\chi}{2} \quad \Rightarrow \text{ epidemic} \qquad (2)$$

whereas if $S_0 < S_c$ there is a skip in the following year.

The above threshold rests on the principle that after a large epidemic the infected population recovers and passes through a period of long-term immunity. A large epidemic is able to exhaust the susceptible pool ($S_0$), and should the latter fall below the critical threshold level ($S_c$), there is a skip—it becomes impossible for a major epidemic to be triggered in the following year. Interestingly, the above criteria (equations (1) and (2)) go beyond the predictions of the classical theory based on the unforced epidemic model[1,27], which sometimes proves to be a misleading guide. For instance, during the skip marked in Fig. 2a, there is a period in which infectives begin to increase rapidly owing to favourable seasonal conditions (high disease transmission). This increase is an indicator that the reproductive number $R_0$ is greater than unity ($R_0 > 1$) and thus, according to the classical theory, suggests a major epidemic is under way. But instead, the growth of infectives is cut short, owing to a change of seasons (diminished disease transmission) which curtails the build-up of the epidemic process, and results in a skip. Whereas predictions based on $R_0$ prove unhelpful here, the criterion of equation (2) is able to correctly differentiate skips from large-scale outbreaks.

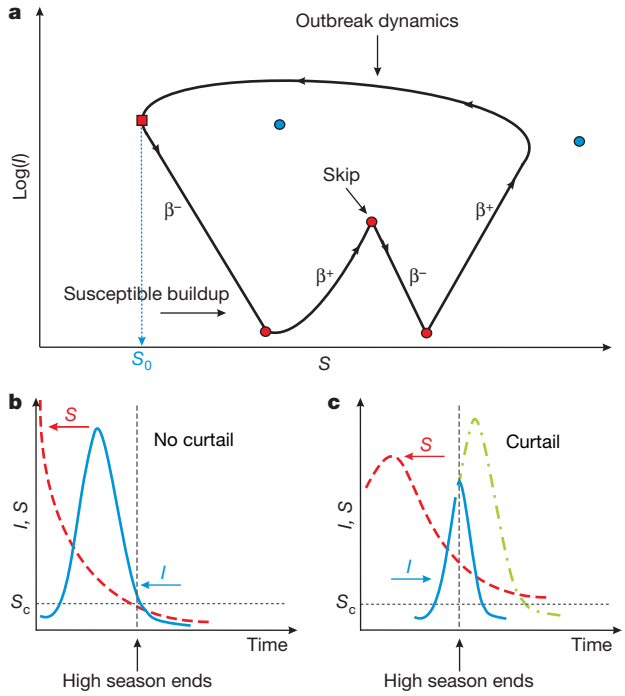


**Figure 2 | Effects of seasonality on population dynamics. a**, Phase plane diagram with the number of infectives $\log(I)$ plotted as a function of susceptible numbers ($S$) for a typical biennial cycle. The trajectory of the SIR model (equation (3)) rotates anti-clockwise around the phase plane. The trajectory is attracted to the quasi-equilibrium associated with each season (each marked as a filled blue circle). As the seasons (and contact rates $\beta^{\pm}$) change, the trajectory is kicked from one equilibrium to the next. The symbols $\beta^+$ and $\beta^-$ are marked on the curve to indicate those periods of time when the contact rates are associated with high and low seasons respectively. In this biennial cycle, an epidemic occurs in the upper part of phase plane, after which susceptibles pass through a minimum ($S_0$, marked by the red square), with a skip occurring in the following year (lower part of phase plane). During a skip, the susceptibles slowly build up, and a small maximum in infective numbers develops one year after the major outbreak. This maximum is prevented from reaching large numbers, as it is curtailed by the change of seasons ($\beta^+ \rightarrow \beta^-$). In contrast to a skip, susceptibles decrease in number during an outbreak. We now consider the relationship between peak outbreak magnitude and initiation time. **b**, An infected individual enters the population early in the high season, and a full scale epidemic develops (solid line). Susceptible numbers fall below the critical level $S_c$. **c**, An infected individual enters the population very late in the high season. The epidemic (solid line) is cut short at the end of the high season, and prevented from reaching its full potential (dashed-dotted line). Susceptible numbers remain above the critical level $S_c$. Although the outbreak is curtailed, it should not be viewed as a skip (as susceptible levels decrease over the epidemic).

The effectiveness of the threshold prediction may be demonstrated through the study of simulated epidemic time series. The seasonally forced SIR model was integrated in the chaotic regime, which advantageously generates time series with skips and variability similar to real world data. The threshold point ($S_c$) may thus be easily checked. Figure 3 plots the time $\tau$ between two successive large-scale epidemics A and B, as a function of the susceptibles $S_0$ left after the first outbreak A. For the given model parameters (Fig. 3 legend), the theoretical critical susceptible threshold ($S_c = 0.031$ from equation (2)) corresponds to the number of susceptibles seen in Fig. 3 that separates the annual dynamics ($\tau \approx 1$) from the biennial dynamics ($\tau \approx 2$) in which there is a skip between two outbreaks. Our formalism provides an exact topological distinction that differentiates a skip from an outbreak, even if small. During a skip, susceptibles always increase in time, whereas during an outbreak they must decrease (Fig. 2 legend). Figure 3 shows explicitly how $S_0$, which characterizes population susceptibility, gives accurate predictions of future outbreaks.

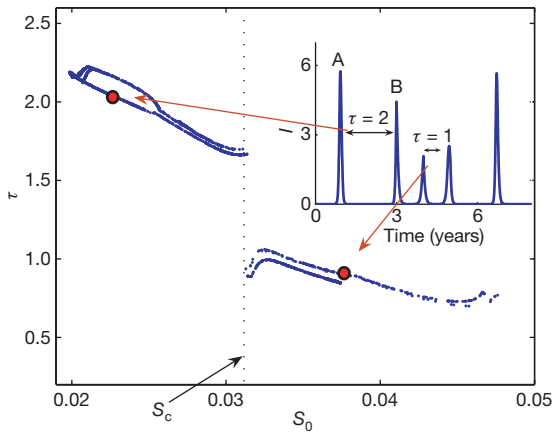


**Figure 3 | Testing the threshold prediction, equation (2).** The forced SIR epidemic model was integrated in the chaotic regime to generate simulated time series of infectives and susceptibles in the population. A typical chaotic time series is displayed in the inset, where the proportion of infectives $I$ is scaled by a factor of $10^{-3}$. Main panel, the time $\tau$ between two successive large-scale epidemics A and B is plotted as a function of the proportion of susceptibles $S_0$ left in the wake of the first epidemic A. To aid visualization, red arrows identify location of specific $\tau$ values found in the time series (inset). To calculate $S_0$, recall that after the peak of a major epidemic the susceptibles $S$ fall in number and eventually build up again due to births. $S_0$ is defined as the number of susceptibles at the local minimum. The theoretical susceptible threshold ($S_c = 0.031$ from equation (2)) corresponds to the susceptible numbers seen in the figure separating annual dynamics ($\tau \approx 1$) from biennial dynamics ($\tau \approx 2$). Parameters for the simulated chaotic regime: $\mu = 0.02$, $\gamma = 66$, $\beta_0 = 1{,}600$, $\delta = 0.18$, $\varepsilon = 10^{-12}$. Forcing is described in Methods, with high and low seasons both half a year in duration.

The relationship between $\tau$ and $S_0$ remains very similar even when the phase and intensity of seasonality undergoes significant random perturbation or for different transmission forms of the function $\beta(t)$ (for example, sinusoidal, step). Similar results are obtained with time series generated by the stochastic TSIR time series model[8,9,25] (Supplementary Information E).

The above model formulation also gives insights as to what might occur if there are shifts in demographic parameters. For example, it has been argued[6,8,9] that the shift from annual to biennial measles dynamics in the UK in the 1940s (Fig. 1) is a consequence of a parallel decline in birth-rate, $\mu$. The threshold criterion (equation (2)) indicates that a decrease in $\mu$ (and its concomitant decrease in available susceptibles) increases the critical susceptible threshold $S_c$ to a level that can prevent an epidemic occurring in the next year. This confirms the verbal arguments and simulations in refs 6, 8 and 9.

The threshold prediction (equation (2)) corroborates conventional epidemiological wisdom[4], which suggests that very large outbreaks should be followed by minor outbreaks or even no outbreaks at all (skips) owing to exhaustion of the susceptible pool $S_0$. However, as we will show below, conventional wisdom cannot always be relied upon. First though, it is important to identify the key factors that have the greatest influence on $S_0$, and thus on the magnitude of the following outbreak. We argue that the phase of the epidemic, or the specific time (for example, month) of the year at which the epidemic achieves a maximum, is an overlooked factor. Our SIR modelling approach provides a natural way to disentangle the complicated relationship between phase and $S_0$ when there is seasonal forcing. The essence of our theoretical results (Supplementary Information D) may be understood through the following simplified sketch. First, consider the case in which there are only two main seasons each year, a 'high' season (high disease transmission) and a 'low' season (low disease transmission). Suppose an infected individual is introduced into a population of susceptibles during the high season. It makes a crucial difference whether the individual enters the population relatively early or late.

First, consider the scenario in which the infected individual is introduced early in the high season and proceeds to initiate an epidemic. This gives plentiful time for the development of a full-scale epidemic (see Fig. 2b). These large protracted epidemics eventually die out, exhausting the susceptible pool ($S_0$) in the process. If $S_0 < S_c$, there are too few susceptibles to fuel an epidemic in the following year. Second, in contrast, should an infected individual enter the susceptible population very late in the high season, there may be little time available for the build up of a large-scale outbreak. Being late, the epidemic is more likely to be affected as the season changes from high to low. The smaller contact rate associated with the low season can act to curtail the epidemic, and cut it short (Fig. 2c). As a result, a large susceptible pool $S_0$ remains. Should $S_0 > S_c$, the number of susceptibles will be enough to trigger an outbreak in the following year. Note that although the epidemic is curtailed, it should not be viewed as a skip (Fig. 2c legend).

The above intuitive argument predicts that for otherwise similar initial conditions the resultant $S_0$ is positively correlated with the entry time of the infected individual. The same can be shown (Supplementary Information D) for the forced SIR model where the phase of the epidemic is directly related to the entry time of infected individuals, and thus positively correlated with the resultant $S_0$. An epidemic that peaks early (low phase) will thus leave small $S_0$ and vice versa.

When this observation is combined with the above threshold theorem, we can immediately see the consequences. Epidemics that occur very early in the season (that is, having low phase) have the potential to exhaust the susceptible pool to a point where $S_0 < S_c$. These epidemics are followed by a skip. Indeed, this proves to be the case in both model and real data. Figure 4 is a plot of the maximum of the following year's outbreak as a function of the phase of the current year's outbreak for four well known time series of measles in four major cities of England and the United States (see Supplementary Information F for other cities and diseases). The plot demonstrates that epidemics peaking early in the year (months 0–3) are generally not followed by large-scale epidemics, but are followed by skips instead. Model time series of infectives undergoing chaotic oscillations show the same pattern (Fig. 4 inset; months 4–6.5). A more detailed analysis of the forced SIR model[28] shows that the later the phase, the larger the next epidemic, as also seen in the analysis of real data in Fig. 4.

It is now possible to understand why large epidemics are not always followed by skips, as conventional wisdom might suggest. Depending on initial conditions, some outbreaks are able to reach large levels despite the fact that they occur relatively late in the high season. These outbreaks will be curtailed when the season changes from high to low. Outbreaks that are curtailed before attaining their potential maximum have the distinguishing feature of being synchronized to the seasonal cycle, as they are all curtailed at the same time—when the season changes. Furthermore, these synchronized outbreaks will have consumed only a fraction of the available susceptible pool. Thus, in the case of the SIR model, all the late synchronized outbreaks are followed by major epidemics in the next year, as shown (in red) in Fig. 4 inset.

Another intriguing outcome of the model concerns the synchronization dynamics of skips. Fine and Clarkson[5] noted that all minor outbreaks in England and Wales arrive relatively late in the school year and end at summer, synchronized to the beginning of the school vacation. The seasonally forced SIR model makes clear why skips are synchronized. As shown in Fig. 2a, all skips in the model occur when the seasons change from high to low and as such infectives change sharply from increasing growth rate to a decreasing one. These curtailed skips must peak at exactly the same time of year. Naturally, when the seasonal change is more gradual, as in the real world, the synchronization will be less exact but the tendency will be strongly apparent. Figure 1b and d makes clear that for the New York and London measles data sets, all of the smaller peaks (skips) occur in the last months of the school season (as marked in red), confirming the synchronization effect.

The analysis reported here is not restricted to childhood epidemics. The above seasonally forced epidemic model is used in a

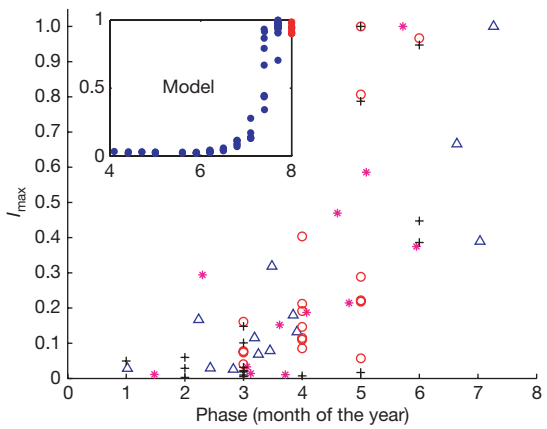


**Figure 4 | The relationship between an outbreak's current phase (month of year) and the maximum number of infectives $I_{max}$ in the following year's outbreak.** Outbreaks that occur early (low phase) are followed in the next year by skips (minor epidemics). Late occurring outbreaks give rise to large epidemics in the following year. Phase relationships are shown for New York (circles), London (triangles), Birmingham (stars) and Baltimore (plus signs) measles time series, using data selected as detailed in Methods after normalization. An extended analysis of these and other measles and mumps data sets is given in Supplementary Information F. Inset, the same analysis is repeated for chaotic model time series (Fig. 3 inset); axes as main panel. All curtailed outbreaks (red) peak at $t = 8$. These synchronized outbreaks (which constitute 20% of outbreaks shown) are all followed in the next year by large epidemics.

range of applications from studies of influenza dynamics[15,16] to models of plant pathogens as agents of bioterrorism[29]. The threshold identified above should have importance in many of these different contexts. The work goes beyond existing theories on the regular and irregular cycles of recurrent diseases, in that it offers new epidemic predictions derived from a widely studied model otherwise considered analytically intractable. Moreover, because of the complex dynamics induced by seasonality, these predictions can differ from expectations obtained from the unforced model. Further work is required to extend the analysis to the case of variable population size, and for conditions of variable birth rates, both of which are recognized as important processes in previous theory of childhood diseases. Predictions based on phase should have particular relevance for newly emerging and re-emerging diseases[30], where time series are too short for rigorous statistical analysis and the epidemiological parameters are extremely difficult to estimate. Yet the theory suggests that useful information can be gained by determining whether an epidemic dies from resource exhaustion or by being curtailed through seasonal change. The latter should be seen as a warning signal for the next year, as population susceptibility and the propensity for an epidemic must both be large. In addition, this work highlights the role of phase as a proxy for population susceptibility. As phase is determined according to the seasonal cycle, the above results imply that monitoring seasonal factors (for example, vector abundance) is imperative in public health management.

## METHODS

**Models.** The classical forced SIR model[1] has the following equations:

$$\dot{S}=\mu-\mu S-\beta(t)\,S(I+\varepsilon);\quad \dot{I}=\beta(t)\,S(I+\varepsilon)-\gamma I-\mu I;\quad \dot{R}=\gamma I-\mu R;\quad (3)$$

where the population is composed of susceptible ($S$), infected ($I$) and recovered ($R$) individuals, and are scaled here as proportions. The rate of birth and mortality is $\mu$, infected individuals recover at rate $\gamma$, and $\varepsilon=10^{-12}$ is a small immigration term[18]. For the case of two seasons each year, the contact rate $\beta(t)$ may be approximated as $\beta^{+}=\beta_0(1+\delta)$ in the high season and as $\beta^{-}=\beta_0(1-\delta)$ in the low season, where $0<\delta<1$ represents the strength of the seasonal forcing. Over time, the seasons change sequentially: high$\rightarrow$low$\rightarrow$high$\rightarrow$low$\rightarrow$ ……

A mathematical analysis of the forced ($\delta>0$) model's epidemic dynamics is given in Supplementary Information A–C and ref. 28. The simulations in ref. 7 also clarify the effects of forcing, but do not develop a language of skips attempted here. For a given $S_0$, it is possible to derive mathematical expressions for the model's orbit in the lower part of phase plane in Fig. 2a, and calculate the resulting number of skips. The analysis uncovers the threshold point separating annual and biennial (or higher-order) dynamics. An intuitive understanding may be gained by removing seasonal forcing ($\delta=0$) altogether. Let $w=\log(I)$, and consider the model's trajectory in the lower part of the $S$–$w$ phase plane. Beginning in the wake of a large epidemic, with $(S,w)=(S_0,w_0)$, equations (3) may be approximated as: $\dot{w}=\beta_0 S-\gamma-\mu$ and $\dot{S}\approx\mu$. Susceptibles build up linearly, $S(t)\approx S_0+\mu t$, and $w(t)$ follows a simple parabola (Supplementary Information C), first descending to very low numbers, and later increasing when the turning point is reached. The recovery time between major epidemics is approximately $t_r=2(\gamma+\mu-\beta_0 S_0)/(\beta_0\mu)$, the time needed for $w(t)$ to return to $w=w_0$. The number of skips is $k\approx t_r/\chi-1$, where $\chi=1-$ year. Rearranging the last equation for $t_r$ gives the maximum level of $S_0$ susceptibles required to generate $k$ consecutive skips, namely $S_c(k)=(\gamma+\mu)/\beta_0-(k+1)\mu\chi/2$. We have shown that the above results hold when forcing ($\delta>0$) is fully taken into account (Supplementary Information B; ref. 28).

**Data analysis.** Measles time series for the US (1928–63, sampled monthly) and the UK (1948–68, sampled weekly) were obtained from ref. 4 and http://www.zoo.ufl.edu/bolker/. In preparing Fig. 4, UK time series were first smoothed using a gaussian kernel as an aid in peak-detection. When testing the effect of the phase of a major epidemic on the following year's peak height, only years having major epidemics are relevant for the analysis. Those years with skips ($\sim$50% of US and $\sim$30% of UK data) were omitted. Likewise, owing to the action of the threshold, the very largest peaks (independent of their phase) were always followed by skips, and hence were also removed from the analysis, although the results obtained were robust to inclusion of these latter points. The final data sets are given in Supplementary Information F. A more refined method for checking the effects of phase would require removing the interaction of peak height altogether. With plentiful data, this could be achieved by examining only a subset of epidemic peaks of a specific height, say $h$, from which a graph of phase versus the next peak's height could be compiled. However, given the limited number of data points, this was impractical for the measles time series, but data-rich model simulations yielded the expected phase relationship, shown in Fig. 4 inset.

**Received 25 July 2006; accepted 10 January 2007.**


1. Anderson, R. M. & May, R. M. *Infectious Diseases of Humans: Dynamics and Control* (Oxford Univ. Press, New York, 1991).
2. Pascual, M. & Dobson, A. Seasonal patterns of infectious diseases. *PLoS Med.* **2,** 18–19 (2005).
3. Altizer, S. *et al.* Seasonality and the dynamics of infectious diseases. *Ecol. Lett.* **9,** 467–484 (2006).
4. London, W. P. & Yorke, J. A. Recurrent outbreaks of measles, chickenpox and mumps. 1. Seasonal variation in contact rates. *Am. J. Epidemiol.* **98,** 453–468 (1973).
5. Fine, P. E. M. & Clarkson, J. A. Measles in England and Wales-I: An analysis of factors underlying seasonal patterns. *Int. J. Epidemiol.* **11,** 5–14 (1982).
6. Earn, D. J. D., Rohani, P., Bolker, B. M. & Grenfell, B. T. A simple model for complex dynamical transitions in epidemics. *Science* **287,** 667–670 (2000).
7. Keeling, M., Rohani, P. & Grenfell, B. T. Seasonally forced disease dynamics explored as switching between attractors. *Physica D* **148,** 317–335 (2001).
8. Bjornstad, O. N., Finkenstadt, B. F. & Grenfell, B. T. Dynamics of measles epidemics: estimating scaling of transmission rates using a time series SIR model. *Ecol. Monogr.* **72,** 169–184 (2002).
9. Finkenstadt, B. F. & Grenfell, B. T. Time series modelling of childhood diseases: a dynamical system approach. *Appl. Stat.* **49,** 187–205 (2000).
10. Olsen, L. F., Truty, G. L. & Schaffer, W. M. Oscillations and chaos in epidemics: a nonlinear dynamic study of six childhood diseases in Copenhagen, Denmark. *Theor. Pop. Biol.* **33,** 344–370 (1988).
11. Schwartz, I. B. & Smith, H. L. Infinite subharmonic bifurcation in an SEIR epidemic model. *J. Math. Biol.* **18,** 233–253 (1983).
12. Aron, J. L. & Schwartz, I. B. Seasonality and period-doubling bifurcations in an epidemic model. *J. Theor. Biol.* **110,** 665–679 (1984).
13. Bolker, B. M. & Grenfell, B. T. Chaos and biological complexity in measles dynamics. *Proc. R. Soc. Lond. B* **251,** 75–81 (1993).
14. Billings, L. & Schwartz, I. B. Exciting chaos with noise: unexpected dynamics in epidemic outbreaks. *J. Math. Biol.* **44,** 31–48 (2002).
15. Andreasen, V. Dynamics of annual influenza A epidemics with immuno-selection. *J. Math. Biol.* **46,** 504–536 (2003).
16. Casagrandi, R., Bolzoni, L., Levin, S. A. & Andreasen, V. The SIRC model and influenza A. *Math. Biosci.* **200,** 152–169 (2006).
17. Dietz, K. The incidence of infectious diseases under the influence of seasonal fluctuations. *Lect. Notes Biomath.* **11,** 1–15 (1976).
18. Engbert, R. & Drepper, F. R. Chance and chaos in population biology – models of recurrent epidemics and food chain dynamics. *Chaos Solitons Fractals* **4,** 1147–1169 (1994).
19. Olsen, L. F. & Schaffer, W. M. Chaos versus noisy periodicity: alternative hypotheses for childhood epidemics. *Science* **249,** 499–504 (1990).
20. Rand, D. A. & Wilson, H. B. Chaotic stochasticity: a ubiquitous source of unpredictability in epidemics. *Proc. R. Soc. Lond. B* **246,** 179–184 (1991).
21. Schaffer, W. M. & Kot, M. Nearly one dimensional dynamics in an epidemic. *J. Theor. Biol.* **112,** 403–427 (1985).
22. Dushoff, J., Plotkin, J. B., Levin, S. A. & Earn, D. J. D. Dynamical resonance can account for seasonality of influenza epidemics. *Proc. Natl Acad. Sci. USA* **48,** 16915–16916 (2004).
23. Shulgin, B., Stone, L. & Agur, Z. Pulse vaccination strategy in the SIR epidemic model. *Bull. Math. Biol.* **60,** 1123–1148 (1998).
24. Huppert, A., Blasius, B., Olinky, R. & Stone, L. A model for seasonal phytoplankton blooms. *J. Theor. Biol.* **236,** 276–290 (2005).
25. Finkenstadt, B. F. & Grenfell, B. T. Empirical determinants of measles metapopulation dynamics in England and Wales. *Proc. R. Soc. Lond. B* **265,** 211–220 (1998).
26. Sugihara, G. & May, R. M. Nonlinear forecasting as a way of distinguishing chaos from measurement error in time-series. *Nature* **344,** 734–741 (1990).
27. Murray, J. D. *Mathematical Biology* 2nd edn (Springer, Berlin, 1989).
28. Olinky, R., Huppert, A. & Stone, L. Thresholds in seasonally forced epidemiological models. *Proc. Natl Acad. Sci. USA* (submitted).
29. Madden, L. V. & Van den Bosch, F. A population-dynamics approach to assess the threat of plant pathogens as biological weapons against annual crops. *Bioscience* **52,** 65–74 (2002).
30. Morens, D. M., Folker, G. K. & Fauci, A. S. The challenge of emerging and re-emerging infectious diseases. *Nature* **430,** 242–249 (2004).


**Supplementary Information** is linked to the online version of the paper at www.nature.com/nature.

**Acknowledgements** We are grateful for the support of the James S. McDonnell Foundation. A.H. was partly supported by the Porter School of Environmental Studies at Tel Aviv University.

**Author Information** Reprints and permissions information is available at www.nature.com/reprints. The authors declare no competing financial interests. Correspondence and requests for materials should be addressed to L.S. (lewi@post.tau.ac.il).